

Non-Lorentzian Rayleigh spectra of bulk homopolymers far above the glass transition

F. Alvarez and J. Colmenero

Departamento de Física de Materiales, Facultad de Química, Apartado 1072, 20080 San Sebastián, Spain

J. Kanetakis* and G. Fytas

Foundation for Research and Technology-Hellas, P.O. Box 1527, 71110 Heraklion, Crete, Greece

(Received 25 January 1994)

Non-Lorentzian depolarized Rayleigh-scattering spectra have been clearly observed by Fabry-Perot interferometry in bulk homopolymers, polyisoprene and 1,4-polybutadiene, far above the glass-transition temperature. We have developed two alternative phenomenological methods for analyzing this kind of spectra. First of all we have used a scattering model function based on the Havriliak-Negami relaxation function which, in fact, is compatible with a Kohlrausch-Williams-Watts relaxation function in the time domain. In the case of polyisoprene, the results obtained by this method are in good agreement with the obtained ones through other different relaxation techniques when a similar method of analysis is applied. Besides, we have extended to the frequency domain the CONTIN algorithm which calculates an apparent distribution function of relaxation times from nonexponential time domain relaxation functions. The results obtained as well as the applicability of both methods are discussed.

I. INTRODUCTION

Fabry-Perot interferometry (FPI) can be employed to analyze the depolarized Rayleigh scattering (DRS) spectrum from viscoelastic media above about 50 MHz and hence at high temperatures far above T_g . In combination with photon correlation spectroscopy (PCS) which covers the time range from 10 μ s to 100 s one can practically cover 14 decades in time using the technique of dynamic light scattering. The DRS spectra of molecular glass-forming liquids have been systematically analyzed in terms of a Lorentzian line-shape function deconvoluted from the instrumental function, which reveals the presence of a single α -relaxation process.^{1,2} By extending the frequency range of the FPI or by using the tandem FPI configuration, an additional much faster process has recently been observed in the molecular glass former ortho-terphenyl.³ The α -relaxation process at high temperatures probed by DRS is characterized by a single relaxation time and follows an Arrhenius temperature dependence, whereas the fast process analyzed in terms of a Lorentzian function is practically temperature independent.

The use of a sum of two Lorentzians has proven successful in analyzing depolarized spectra of polymer/diluent systems.⁴⁻⁶ In this case the single fast and slow relaxation times correspond, respectively, to reorientation of the free diluent and the diluent bound by the polymer molecules.

The finding of single relaxation time processes at high temperatures is in accord with theoretical modes (coupling model,⁷ phase-space model,⁸ two-spin facilitated model⁹) which predict that the distribution of relaxation times is temperature dependent. Besides DRS, dielectric relaxation (DS) measurements may also be employed to probe orientational motions at high temperatures. The relaxation times obtained by both techniques¹ are in good

agreement for the molecular glass former di-2-ethylhexyl phthalate.

Turning to bulk homopolymers, the DS data over the frequency range 1 MHz to 1 GHz cannot be described unless a distribution of relaxation times is invoked, and which persists at high temperatures.^{10,11} In addition to DS, time-resolved optical experiments have been employed to indirectly probe polymer dynamics in a wide temperature range above T_g , by following the reorientational motion of a probe chromophore embedded in the bulk polymer¹² or of a chromophore covalently attached to the polymer chain.^{13,14} The fluorescence anisotropy decay functions were found to be nonexponential.¹⁴ Another experimental technique to probe local segmental dynamics associated with the α relaxation in polymer glass formers far above T_g is quasielastic neutron scattering (QENS). In the case of time domain QENS, recent results obtained by neutron spin echo¹⁵⁻¹⁷ (NSE) have proved that the dynamic structure factor $S(Q, t)$ at wave vector Q over the time range 2 ns–2 ps can be represented by the well known Kohlrausch-Williams-Watts (KWW) function. For polyisoprene, a value of the shape parameter of the KWW function, $\beta \cong 0.4$, has been reported¹⁷ from NSE in agreement with DS data. This agreement further encompasses a common temperature dependence which is the same found by rheological measurements. On the other hand, in a series of recent papers,¹⁸⁻²⁰ Colmenero, and co-workers have shown that the incoherent QENS curves $S(Q, \omega)$ in a frequency range about 10^8 Hz to 10^{10} Hz and in a Q range roughly between 0.1 and 3 \AA^{-1} are non-Lorentzian for the three polymers investigated. They have also shown that these results can be well interpreted by assuming a KWW intermediate scattering function, $I(Q, t)$, with β values which appear to be hardly Q and temperature dependent. These β values are similar to the obtained ones through dielectric measurements. Moreover the relaxation times

obtained from both QENS and DS measurements show the same temperature dependence. All of these results indicate that segmental relaxation as probed by QENS and orientational relaxation as observed by DS are of the same origin. Recent molecular-dynamics simulations of a united-atom polyethylene model²¹ also give additional support to this conclusion.

The question arises as to whether DRS spectra at high T can be adequately described by a Lorentzian function (single-relaxation process) or a distribution of relaxation times is necessary, as DS and NSE data suggest. This paper deals with the analysis of the non-Lorentzian FPI-DRS spectra observed in bulk homopolymers at high T . Non-Lorentzian behaviors have also been reported for molecular glasses.²² Two different methods of analysis are presented here. According to the first method, a procedure will be shown which assumes a Havriliak-Negami (HN) relaxation function which is supposed to describe the experimental spectra, just in the same way HN functions are supposed to be good descriptions of the experimental data measured by other frequency-domain techniques (such as dielectric and mechanical) at lower temperatures closer to T_g . The second method of analysis that we introduce here consists on trying to extract directly from the experimental DRS curves an apparent distribution function of the relaxation times in the way the CONTIN program²³ calculates such a distribution function from time domain PCS measurements through an inverse Laplace transformation procedure.

II. EXPERIMENTAL

A. Depolarized Rayleigh scattering (DRS)

The depolarized light-scattering spectra $I_{VH}(\omega)$ were obtained at a scattering angle of 90° using a single-mode argon-ion laser (Spectra Physics 2020) delivering an average power of 150 mW at 488 nm. The incident beam was vertically polarized relative to the scattering plane by means of a Glan polarizer with an extinction coefficient of 10^{-6} . The scattered light was collected through a Glan-Thompson polarizer with an extinction coefficient better than 10^{-7} , and frequency analyzed with a piezoelectrically driven Fabry-Perot interferometer (Burleigh RC-110). The mirrors were 50 mm in diameter with a flatness of $\lambda/200$ and reflectivity of about 0.98. The typical scan rate of the single pass interferometer was 0.5 sweeps/s. Five free spectral ranges (FSR), 4.5, 6.31, 7.31, 12, and 16.96 GHz were used and the typical operating finesse obtained was better than 60. A stabilization system (Burleigh DAS-10) was used to keep the position of the Rayleigh peak fixed and maintain maximum finesse. The scattered light, after passing through the interferometer, was detected by a photomultiplier (EMI 9863); a narrow band interference filter was used to reject fluorescence. Following a repetitive averaging, two spectral orders were stored in a 2048 channel multichannel analyzer (Canberra, Series 35plus) and transferred to a VAX main-frame computer for analysis.

B. Materials

Three 1,4-polyisoprene (PI) samples coded PI 1, PI 2, and PI 3, and a 1,4-polybutadiene (PB) sample have been used in this study. The characteristics of the four samples are summarized in Table I. The 1,4-polyisoprene samples had the following microstructures. PI 1: 95% (1,4) and 5% (3,4); PI 2: 66% cis-1,4, 27% trans-1,4, and 7% vinyl-3,4; PI 3: 68% cis-1,4, 25% trans-1,4, and 7% vinyl-3,4. The 1,4-polybutadiene sample (PB) had a microstructure 41% cis-1,4, 53% trans-1,4, and 6% vinyl-1,2. The PI 1, PI 2, and PB samples were synthesized at Exxon Chemical Co., NI, and were kindly donated by Professor N. Hadjichristidis. The PI 3 sample (Polysciences) and kindly donated by Professor M. D. Ediger. Dust-free samples were prepared by filtering the homopolymers or their solutions into dedusted light-scattering cells following the procedure described elsewhere.²⁴

III. ANALYSIS IN TERMS OF A HAVRILIAK-NEGAMI FUNCTION

In a first approximation to the problem we consider the possibility that the experimental depolarized spectra might be described by means of a Havriliak-Negami (HN) relaxation function²⁵ convoluted with the instrumental function of the interferometer. The HN function has been widely used to describe data from techniques which act in the frequency domain like dielectric spectroscopy,^{11,26} mechanical relaxation,²⁰ and recently NMR and QENS.¹⁸⁻²⁰ In previous papers^{27,28} some of us showed the interconnections between this function and the Kohlrausch-Williams-Watts (KWW) function $\varphi(t) = \exp(-t/\tau_{KWW})^\beta$, which is also widely used for the representation of the dynamics around the glass-liquid transition.²⁹ The theoretical power spectrum $S(\omega)$ of the depolarized Rayleigh experiment can then be described in terms of the imaginary part of the HN function.

$$S(\omega) = -\frac{1}{\omega} \operatorname{Im} \left[\frac{1}{[1 + (i\omega\tau)^\alpha]^\gamma} \right] \quad (1)$$

where τ is a characteristic relaxation time and α, γ are shape parameters ranging between 0 and 1.

The theoretical expression [Eq. (1)] was convoluted with the instrumental function and two neighboring interferometric orders were also taken into account. The consistency of the obtained values was also treated by the comparison among measurements with different free spectral ranges (FSR).

In Fig. 1 the depolarized Rayleigh spectrum of poly-

TABLE I. Sample characteristics.

Sample	M_w	M_w/M_N	$T_g, ^\circ\text{C}$
PI 1	1 030	1.10	-66.6 ^a
PI 2	2 350	1.10	-69 ^b
PI 3	34 000	1.04	
PB	2 660	1.13	

^aHeating rate 20 K/min.

^bHeating rate 5 K/min.

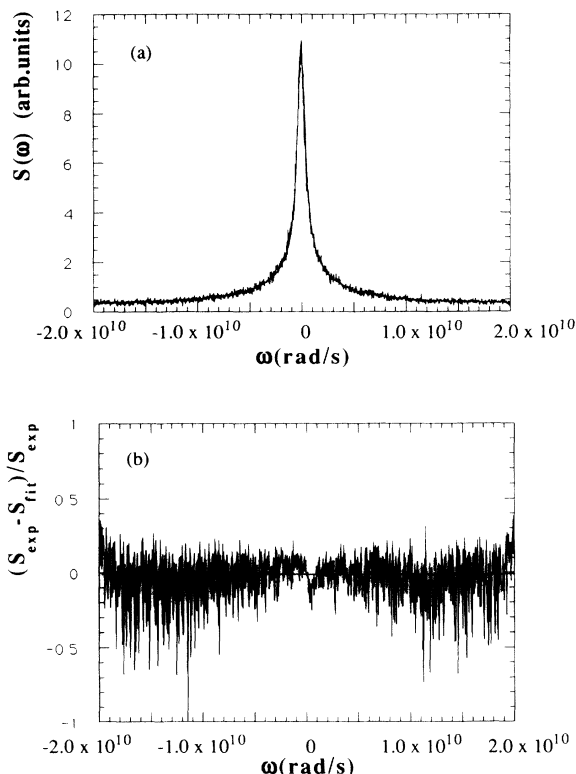


FIG. 1. (a) Plot of the depolarized spectrum of PI as measured with the technique of DRS at the temperature of 80°C with a free spectral range of 6.313 GHz and its fit by means of a HN function of the following parameters $\alpha=0.72$, $\gamma=0.49$, and $\log_{10}\tau=-9.6$ (in seconds). (b) Residual plot of (a).

isoprene sample PI3 measured at $T=80^\circ\text{C}$ and $\text{FSR}=6.31$ GHz is shown, and analyzed in terms of a HN function following the procedure just mentioned. The HN parameters [$\alpha=0.72$, $\gamma=0.49$, and $\log_{10}\tau=-9.6$ (in seconds) in the case of $T=80^\circ\text{C}$] thus obtained were found to be compatible with a Kohlrausch-Williams-Watts-shaped relaxation function in the time domain and, consequently, were transformed to the values of τ_{KWW} and β , in the way described in Refs. 25 and 26. The value of the β parameter thus obtained ($\beta=0.40$) compares well with those obtained earlier either from dielectric¹⁰ or from PCS.³⁰ For the polyisoprene samples PI1 and PI2 this analysis gives the same set of HN parameters and thus it is insensitive to molecular weight variations, as expected for relaxation times of segmental motions. As it can be seen in the residual plot (calculated as the difference between the model function and the experimental data, over the experimental spectra) the quality of the fitting is high and no significant structure can be appreciated in the residuals. For comparison, and in order to show explicitly the non-Lorentzian feature of the spectrum, we plot in Fig. 2 the best Lorentzian fit, convoluted with the instrumental function, including a baseline. As one can observe, in this case the model function is not able to describe the experimental data, as it is obviously displayed in the residuals plot.

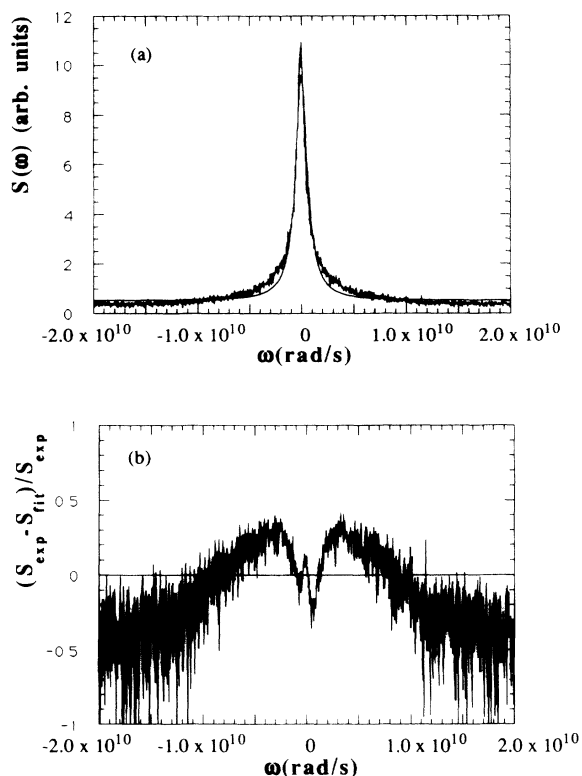


FIG. 2. (a) Plot of the same data of Fig. 1(a) and the attempt to fit it by means of a Lorentzian plus a baseline. (b) Residual plot of (a).

In order to test if the relaxation times obtained by following this procedure compare well with the corresponding ones to other techniques, we plot in Fig. 3 the relaxation times of polyisoprene obtained from DRS by this method together with previously reported results from different experimental techniques, namely, DS,¹⁰ time-

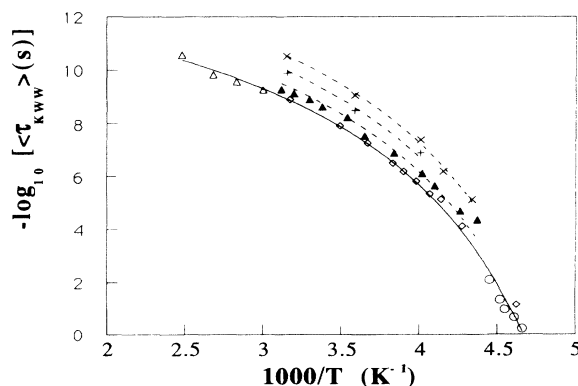


FIG. 3. Logarithmic representation of the $\langle\tau_{\text{KWW}}\rangle = \tau_{\text{KWW}}/\beta\Gamma(1/\beta)$ for the characteristic relaxation times as obtained from the different techniques mentioned in the text. \triangle are DRS data, \diamond DS data, and \circ PCS data. These data are used to obtain a single VF expression. This same VF is shifted through the TRS data (solid triangles) and NSF data (+ and \times). The + correspond to a wave vector of 1.44 \AA^{-1} and the \times to a wave vector of 1.92 \AA^{-1} .

resolved spectroscopy (TRS),¹² NSE,¹⁷ and PCS.³⁰ Two different sets of NSE times are plotted corresponding to different Q values. All relaxation times have been converted to correspond to the same magnitude, namely, the average relaxation time, $\langle \tau_{\text{kww}} \rangle = \tau_{\text{kww}} / \beta \Gamma(1/\beta)$. A pertinent feature of Fig. 3 is the good agreement between our DRS fitting values and the PCS (in the VH mode³⁰) and DS times extracted in this consistent way in the whole temperature region from close to T_g to well above T_g . This result is even more relevant if we take into account that these techniques have very different operating principles. Close to T_g , PCS measures the depolarized correlation functions in the time domain,²⁸ whereas at high T , the FPI technique explores the depolarized spectra in the frequency domain. On the other hand, the DRS and DS techniques probe the polyisoprene segmental dynamics through the optical anisotropy and dipole moment, respectively. Hence these techniques are sensitive to orientational motions. Good agreement between the orientational times from DRS and DS has also been found in molecular glass formers¹ at high T and bulk polymers^{11,24} at low T , close to T_g . This appears to be in contradiction with the theoretical prediction³¹ that far above T_g , the ratio of the orientation times for isotropic rotational diffusion $\tau(l=1)/\tau(l=2)=3$, where $\tau(l)$ is the single-particle orientation time for the l th order spherical harmonic, obtained from DS ($l=1$) and DRS ($l=2$).

The τ values as obtained by DRS and DS are found to conform to the Vogel-Fulcher-Tamman-Hesse (VFTH) expression

$$\tau = \tau_0 \exp \left[\frac{B}{T - T_0} \right]. \quad (2)$$

A nonlinear least-squares fit of Eq. (2) to the DRS (FPI, PCS) and DS data of the Fig. 3 yields $\log_{10}\tau_0 = -12.8$ (τ_0 in seconds), $B = 1352$ K, and $T_0 = 168$ K, values which compare fairly well with $B = 1050$ K, $T_0 = 170$ K reported from the fit of the DS data only.¹⁰ A universal fit of the relaxation data to Eq. (2) suggests that these relaxation times correspond to the primary glass-rubber transition or the α process. Furthermore, the values of the NSE relaxation times¹⁷ also plotted in Fig. 3 for two different wavevectors ($1.92, 1.44 \text{ \AA}^{-1}$) are smaller than those obtained from the other techniques and increase by lowering the Q value. These features are expected since NSE can probe segmental motion at local scale shorter than the correlation length associated with the dielectric α process. However, the temperature dependence exhibited by the NSE data and the orientation times is compatible, as can be seen in the figure, where we have plotted dashed lines through the NSE data corresponding to VFTH expressions of the same B and T_0 values corresponding to the FPI, DS, and PCS data. Moreover fit of the NSE data¹⁷ to the KWW function yields $\beta \approx 0.39$, in agreement with PCS (Ref. 28) and DS (Ref. 10). Notwithstanding, this feature is not that clear concerning the data from the TRS technique, which seem to evolve similarly with respect to the temperature, but fall aside the Vogel-Fulcher (VF) curve defined by the FPI, PCS, and DS techniques.

From the theoretical point of view, the dynamic rotational isomeric state model³⁰ applied in the case of polyisoprene at temperatures in the vicinity of T_g , indicates that the distribution parameter β of the KWW function as extracted from PCS and DS data is reproduced if the kinetic segment consisting of a few repeat units relaxes cooperatively in the presence of free volume fluctuations of the environment.

Furthermore, recent molecular dynamics³¹ of realistic polyethylene chains in the bulk state has revealed significant interchains effects on the local orientation dynamics in the ns time region far above T_g . The orientation correlation functions for vectors along and perpendicular to the chain axes are not exponential and are characterized by very different relaxation rates and ratios τ_1/τ_2 (for the first- and second-order correlation functions). Based on this simulation, the similarities between DRS ($l=2$) and DS ($l=1$) orientation relaxation functions of different unit vectors in PI rather favor inter-chain effects on the orientation of few repeat chain units.³⁰ The latter connectivity constraint is absent in molecular viscoelastic fluids.

We have also used this method of analysis to study the experimental DRS spectra measured on a sample of bulk 1,4-poly(butadiene), PB which main characteristics are depicted in Table I. Thus, in Fig. 4 we plot the result obtained by following this procedure of analysis on the

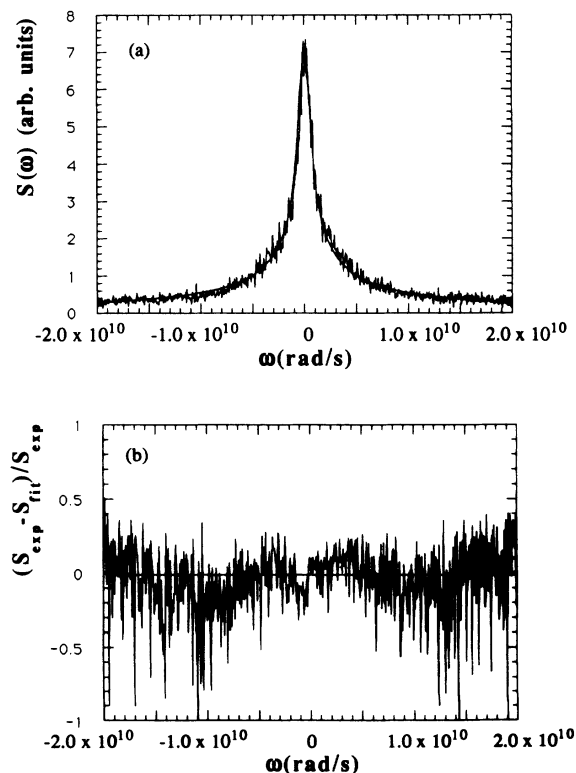


FIG. 4. (a) Free fit of the depolarized spectrum of 1,4-PB recorded at 95°C with a FSR of 12 GHz with the following parameters $\alpha=1$, $\gamma=0.55$, and $\log_{10}\tau = -9.9$ (in seconds). (b) Residual plot of (a).

spectrum measured at 95 °C with a free spectral range of 12 GHz.

The β value one obtains when allowing this free fitting is higher ($\beta=0.65$) than the one that could be expected. This could perhaps be explained in the sense that this difference might be due to the larger amount of noise arising from the lower optical anisotropy per monomer of 1,4-PB compared to PI ($\gamma^2=4-12 \text{ \AA}^6$). Finally, it is noteworthy that, even though one must recognize that, in this case the data are not perfectly described by this method of analysis, the fitting is still much better than the one obtained by assuming a Lorentzian function, which is definitely not able to reproduce the experimental spectra.

We do not present here a relaxation time plot for PB similar to the one shown in Fig. 3 for PI due to the difficulty of performing a unified analysis in this case, since the different types of analysis used on other techniques, and the lack of information from some of them, do not allow the calculation of a relaxation time defined in the same way for all techniques.

IV. ANALYSIS BASED ON THE INVERSE LAPLACE TRANSFORMATION IN THE FREQUENCY DOMAIN

Once checked the possibility of interpreting the DRS data through a HN relaxation function, we may try to investigate another possible procedure for analyzing the non-Lorentzian behavior of DRS spectra without assuming any predetermined functional form for the relaxation function. The way followed by us consisted on trying to extract directly from the experimental DRS curves an apparent distribution function of the relaxation times in the way the CONTIN program²³ calculates such a distribution function from time domain PCS measurements through an inverse Laplace transformation procedure. The reason of doing so does not lie solely on the arbitrariness of assuming an empirical fitting model like the HN one which has no solid theoretical basis. Even if this HN model could be considered to be valid to represent the dynamical relaxation process, the possibility of having more than a single process relaxing in the Fabry-Perot window should be taken into account.

Another point of interest in the searching for the possibility of extracting a distribution of relaxation times out of the experimental data, is derived from the fact, that if we are able to do so, we can obtain a unitary analysis all along the dynamical scale covering dielectric (both in the frequency and time domains), PCS, mechanical, and DRS measurements. As one can see these are the most frequency employed techniques aimed to study the broad dynamical range covered by the glass-transition relaxation in glass-forming liquids.

As it is widely known, the standard CONTIN program is used to obtain a continuous distribution of relaxation times out of a relaxation function defined in the time domain. This is done by considering the relaxation function as a continuous sum of exponentials. An equivalent scattering relaxation function in the frequency domain should be described by the same continuous distribution of relaxation times, but now considering a continuous

sum of Lorentzians. In this case the corresponding model function which should give account of the dynamics monitored by the technique of DRS should be given by the following expression:

$$S_m(\omega) = \int_0^\infty \rho(\tau) \frac{\tau}{1 + \omega^2 \tau^2} d\tau, \quad (3)$$

where $\rho(\tau)$ is a normalized distribution function:

$$\int_0^\infty \rho(\tau) d\tau = 1. \quad (4)$$

This model function, $S(\omega)$ would directly describe the experimental data in an ideal experiment in which the Fabry-Perot interferometer would have an instrumental function corresponding to a δ function. However, in the actual experiment, the resolution of the apparatus is not that high and one must perform a convolution with the measured instrumental function of the interferometer in order to describe the real data accordingly to the following expression:

$$S_{\text{exp}}(\omega) = \int_{-\infty}^\infty S_m(\omega') I(\omega' - \omega) d\omega', \quad (5)$$

where $I(\omega)$ stands for the instrumental or resolution function of the Fabry-Perot interferometer.

Due to the overlap of the neighboring interferometric orders, the model function should be given by

$$S_m(\omega) = \int_0^\infty \rho(\tau) \left[\frac{\tau}{1 + \omega^2 \tau^2} + \frac{\tau}{1 + (\omega - F')^2 \tau^2} + \frac{\tau}{1 + (\omega + F')^2 \tau^2} \right] d\tau, \quad (6)$$

where $F' = 2\pi F$, F being the free spectral range used in the recording of the measurements. Let us comment that the instrumental function of the interferometer is fitted by means of the sum of a Lorentzian plus a Gaussian functions. It is also noteworthy to say that this effect of the neighboring interferometric orders could be diminished (or rather suppressed) by utilizing a tandem Fabry-Perot.³

Thus, starting from $S_{\text{exp}}(\omega)$ and $I(\omega)$, by following the previous equations, we were able to modify the standard CONTIN in order that with these inputs we could obtain distributions of relaxation times $\rho(\tau)$ [or, rather $\rho(\ln\tau)$] and their corresponding fittings as the output of the program. Once this distribution of relaxation times is obtained it can be integrated in order to obtain the relaxation function either in the time or in the frequency domains. Then, these functions can be treated in the usual standard ways and be fitted either with a KWW function (in the time domain) or with a HN function (in the frequency domain).

We will present first the results obtained on PB with this method. Thus, we show in Fig. 5 the result that we obtained by following this procedure on a spectrum of 1, 4-polybutadiene measured at 95 °C with a free spectral range of 12 GHz.

As one can appreciate the quality of the fit is much higher in this case than in the previous analysis as it can be estimated from the graphics, where a comparative plot

of the experimental data together with the fitting corresponding to the calculated distribution of relaxation times, and the residuals plot are shown. It is also important to say that, although this example we have shown in Fig. 5 is the corresponding one to the final chosen solution of our modified CONTIN version, we must note that this solution is not a unique one. This is so because the problem is not a well-defined one, but an ill-conditioned one. The author of the original CONTIN in the time domain,²³ Provencher, advises the user to look for the physically meaningful solution in the output list and not to take blindly the one chosen by the program (the same

applies for our frequency version). A clear example of this is the case of the analysis of a bimodal solution. If the size of the two sets of particles is not very different, it is very likely that CONTIN takes a unimodal solution as the chosen one for the sake of parsimony. Nevertheless, several trial solutions are listed in the output, and one of them corresponds to the correct bimodal solution.

In the following we show an alternative solution to Fig. 5 which also appears in the output list, and its corresponding fit to the same experimental data. As it can be appreciated this fit is as acceptable as the one in Fig. 5. This indicates that different distributions can yield very similar fittings. Thus, it can be seen from Fig. 6 that the spectrum might be fitted with a single distributed process.

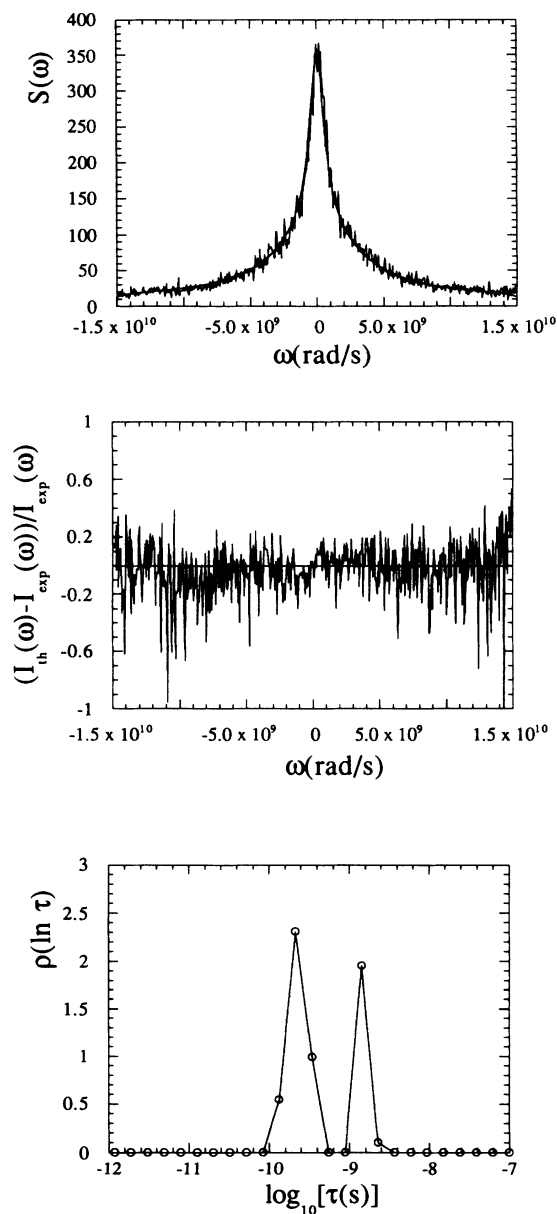


FIG. 5. Experimental spectrum of 1,4-PB recorded at 95 °C with a FSR of 12 GHz and its fit with the distribution of relaxation times (as calculated as explained in the text), shown in the lower graphic. The middle one stands for the residual plot of the fitting.

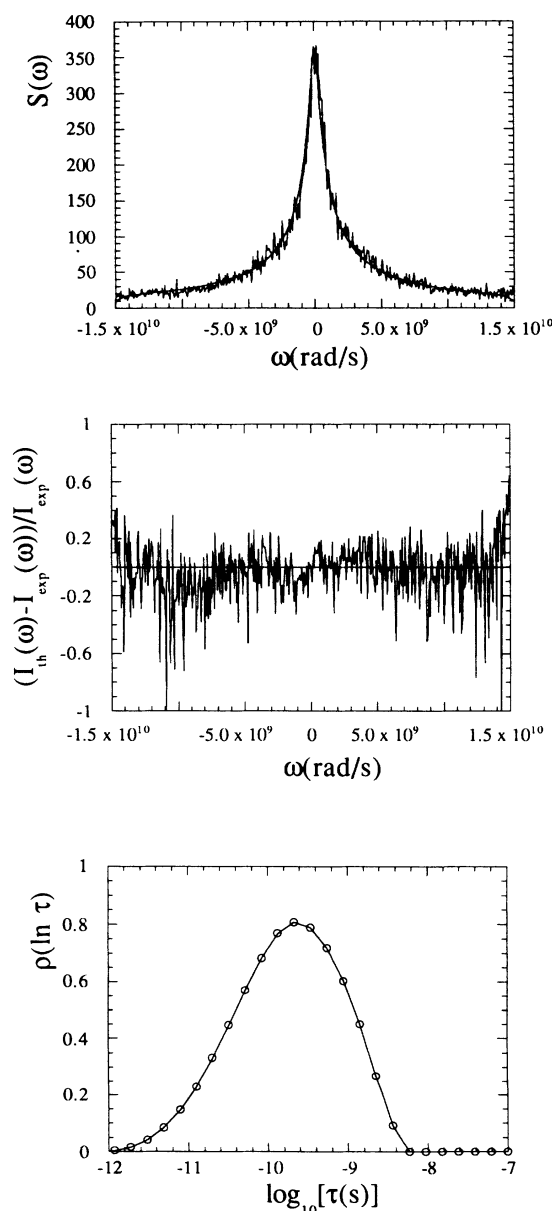


FIG. 6. The same as in Fig. 5 for the alternative distribution shown in the lower graphic.

Nevertheless, when one applies this method to the spectrum of the more optically anisotropic PI we had previously analyzed in terms of a HN function, the following results are found. The chosen solution of our modified CONTIN version is plotted in Fig. 7, where it can be seen that the program resolves two peaks of different width. In this case, when one inspects the possible solutions there is not among them a monomodal one which is able to fit the data. Notwithstanding, the solution in Fig. 8, which is also able to fit the data, give us a hint that a peak-constrained analysis could yield a monomodal solution, according to the result we obtained in our previous

analysis. However, in any case the non-Lorentzian feature of the spectrum is evident.

V. CONCLUSIONS

We have introduced here two types of analysis for the non-Lorentzian spectra of bulk homopolymers as measured by the DRS technique far above T_g . The first analysis is based upon the assumption that the experimental spectra are describable by means of the HN function, just in the same way this empirical function is used to parametrize the experimental results from other techniques acting in the time domain, such as dielectric and mechanical techniques.

We have shown that the results thus obtained for the

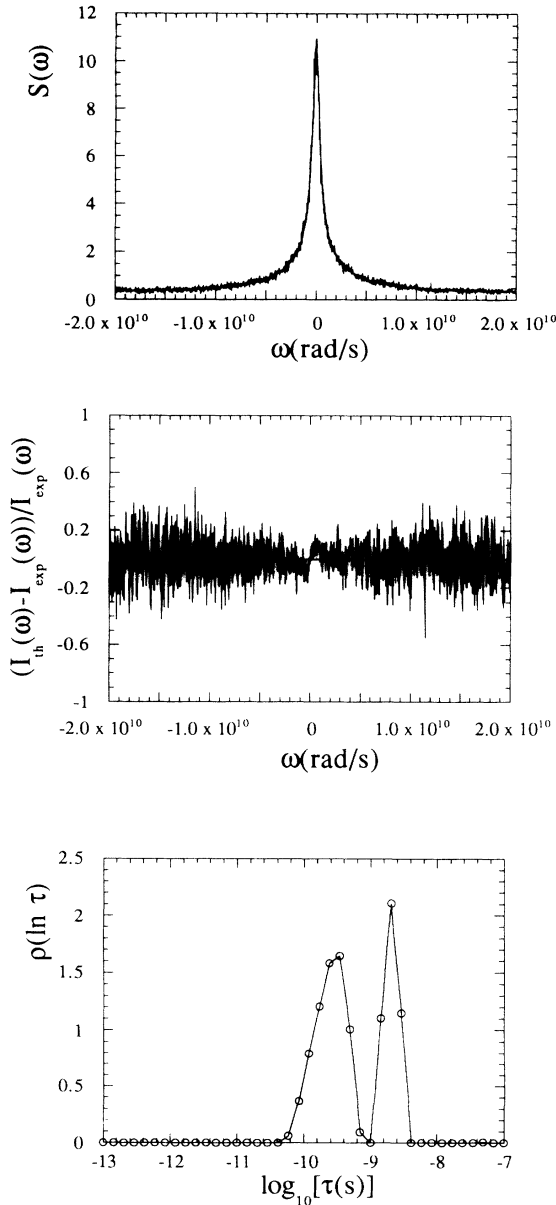


FIG. 7. Experimental spectrum of PI recorded at 80°C with a FSR of 63.13 GHz and its fit with the distribution of relaxation times (as calculated as explained in the text), shown in the lower graphic. The middle one stands for the residual plot of the fitting.

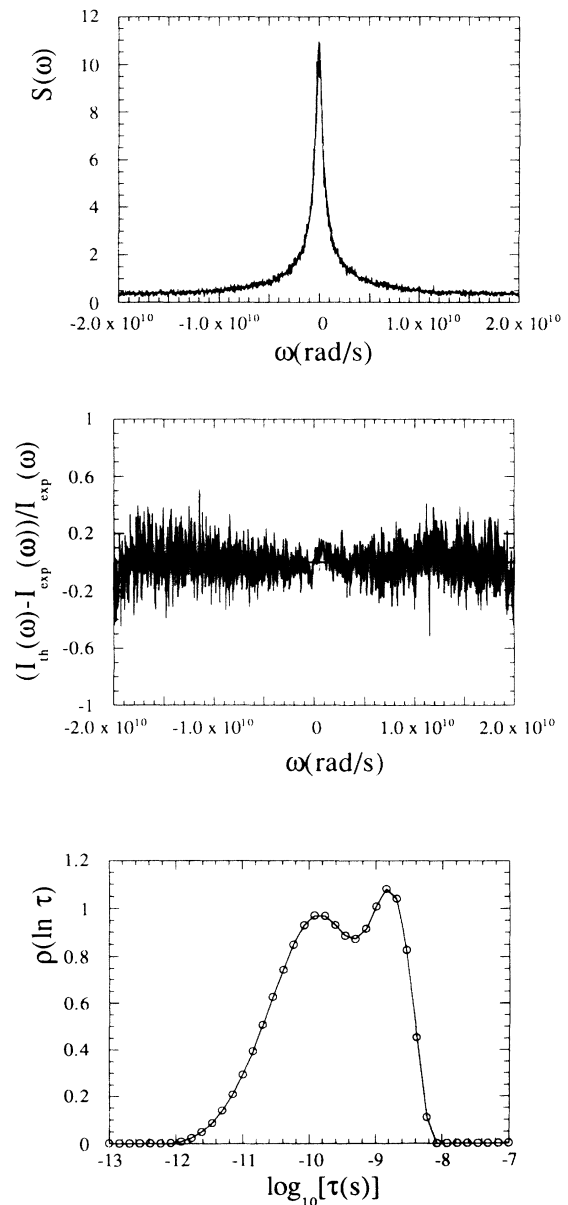


FIG. 8. The same as the Fig. 7 for the alternative distribution shown in the lower graphic.

analysis of DRS (FPI) spectra at high temperatures when compared in the same grounds with results from DRS (PCS) and dielectric measurements at much lower temperatures close to T_g can conform to a single VFTH expression for the PI bulk homopolymer. Moreover, the shape parameters are coincident throughout all the wide interval of temperature. However, in the case of PB, although we also detect a clear non-Lorentzian behavior, the β values obtained are higher than the corresponding ones to lower temperature (lower frequencies) measurements.

The second type of analysis consists on extracting directly from the experimental DRS curves an apparent distribution function of the relaxation times in the way the well known CONTIN program calculates such a distribution function from time domain PCS measurements through an inverse Laplace transformation procedure.

Although as we have shown, the mathematical problem of obtaining a distribution of relaxation times is an ill-posed problem, and although different distributions can be equally valid to describe the experimental data, the non-Lorentzian character of the experimental data is a pertinent feature of the measurements performed by this technique on bulk polymers. This is supported by the fact that the program we use is able to resolve a single Lorentzian convoluted with the instrumental function of the interferometer.

ACKNOWLEDGMENTS

The authors acknowledge financial support from EC, HCM-Network project contract ERBCHRXCT920009. J.C. and F.A. also acknowledge partial financial support from Gipuzkoako Foru Aldundia.

*Present address: Institut für Physikalische Chemie der Universität Mainz, Jakob-Welder-Weg 15, W-6500, Mainz, Germany.

- ¹G. Floudas, J. S. Higgins, and G. Fytas, *J. Chem. Phys.* **96**, 7672 (1992).
- ²Y. Higashigaki and C. H. Wang, *J. Chem. Phys.* **74**, 3175 (1981).
- ³W. Steffen, A. Patkowski, G. Meier, and E. W. Fischer, *J. Chem. Phys.* **96**, 4171 (1992).
- ⁴A. C. Ouano and R. Pecora, *Macromolecules* **13**, 1173 (1980).
- ⁵G. Fytas, A. Rizos, G. Floudas, and T. P. Lodge, *J. Chem. Phys.* **93**, 5096 (1990).
- ⁶G. Floudas, G. Fytas, and W. Brown, *J. Chem. Phys.* **96**, 2164 (1992).
- ⁷K. L. Ngai, R. W. Rendell, A. K. Rojagopal, and S. Teitler, *Ann. N. Y. Acad. Sci.* **484**, 150 (1986).
- ⁸L. A. Campell, J.-M. Flesselles, R. Jullien, and R. Botet, *Phys. Rev. B* **37**, 3825 (1988).
- ⁹G. H. Fredrickson and S. A. Brawer, *J. Chem. Phys.* **84**, 3351 (1986).
- ¹⁰D. Boese and F. Kremer, *Macromolecules* **23**, 829 (1990).
- ¹¹D. Boese, B. Momper, G. Meier, F. Kremer, J.-U. Hagenah, and E. W. Fischer, *Macromolecules* **22**, 4416 (1989).
- ¹²P. D. Hyde and M. D. Ediger, *Macromolecules* **22**, 1510 (1989).
- ¹³P. D. Hyde, M. D. Ediger, T. Kitano, and K. Ito, *Macromolecules* **22**, 2253 (1989).
- ¹⁴J. L. Viovy, L. Monnerie, and F. Merola, *Macromolecules* **18**, 1130 (1985).
- ¹⁵D. Richter, B. Frick, and B. Farago, *Phys. Rev. Lett.* **61**, 2465 (1988).
- ¹⁶B. Frick, B. Farago, and D. Richter, *Phys. Rev. Lett.* **64**, 2921 (1990).
- ¹⁷R. Zorn, D. Richter, B. Farago, B. Frick, F. Kremer, U. Kirst, and L. J. Fetters, *Physica B* **180**, 534 (1992).
- ¹⁸J. Colmenero, A. Alegría, J. M. Alberdi, F. Alvarez, and B. Frick, *Phys. Rev. B* **44**, 7321 (1991).
- ¹⁹J. Colmenero, A. Alegría, A. Arbe, and B. Frick, *Phys. Rev. Lett.* **69**, 478 (1992).
- ²⁰J. Colmenero, A. Alegría, A. Arbe, and B. Frick, *Physica B* **182**, 369 (1992).
- ²¹R. J. Roe, *J. Non-Cryst. Solids* (to be published).
- ²²G. Li, W. M. Du, X. K. Chen, and H. Z. Cummins, *N. J. Tao, Phys. Rev. A* **45**, 3867 (1992).
- ²³S. W. Provencher, *Comput. Phys. Commun.* **27**, 213 (1982).
- ²⁴J. Kanetakis, G. Fytas, and N. Hadjichristidis, *Macromolecules* **24**, 1806 (1991).
- ²⁵S. Havriliak and S. Negami, *Polymer* **8**, 161 (1967).
- ²⁶A. Alegría, J. Colmenero, J. J. del Val, and J. M. Barandiarán, *Polymer* **26**, 913 (1985).
- ²⁷F. Alvarez, A. Alegría, and J. Colmenero, *Phys. Rev. B* **44**, 7306 (1991).
- ²⁸F. Alvarez, A. Alegría, and J. Colmenero, *Phys. Rev. B* **47**, 125 (1993).
- ²⁹See, for example, *Polymer Motion in Dense Systems*, edited by D. Richter and T. Springer (Springer-Verlag, Berlin, 1988).
- ³⁰J. Kanetakis, G. Fytas, F. Kremer, and T. Pakula, *Macromolecules* **25**, 3484 (1992).
- ³¹D. Kivelson and S. A. Kivelson, *J. Chem. Phys.* **90**, 4464 (1989).